SYNTHESIS OF NANOSCALEVATERITE $CaCO_3$ IN W/O MICROEMULSION WITH THE REGULATION OF POLYASPARTIC ACID

P. YAN, X. SU, Y. LU, S. YANG*
School of Chemistry and Material Sciences, Heilongjiang University, Harbin 150080, China

A complex method was used to synthesize nanoscale vaterite $CaCO_3$ by the addition of polyaspartic acid (PASP) into W/O microemulsion to control the crystal shape and particle size. The samples synthesized by using different concentration of reactant and PASP were characterized by XRD, SEM, TEM, N_2 adsorption–desorption and FTIR. The results show that the sample prepared by the addition of 2.5 mg/ml PASP in the 0.5 M reactant system exhibited superior property: nanoparticles size was ca. 50 nm, pore sized distribution was mainly around 40-60 nm and the surface area and mesoporous volume were 27.012 m^2/g and 0.15 cm^3/g, respectively. The possible precipitation process of the nanometer vaterite $CaCO_3$ in the complex system was also discussion. This study will provide a potential method of the combination of the theory of biomineralization and microemulsion.

(Received April 20, 2016; Accepted June 21, 2016)

Keywords: Nanoscalevaterite; Calcium carbonate; W/O microemulsion; polyaspartic acid;

1. Introduction

Calcium carbonate ($CaCO_3$) with nanometer dimensions has been regarded as an important class of materials in industry, medicine and environment. It has a wide range of application, such as capsule agents for drug delivery, filters, coatings, chemical catalysis and templates for functional architectural composite materials because of their unique structural and excellent surface properties[1-5]. The performance of $CaCO_3$ materials are closely related to the crystal shape and particle size, which can be modified by biomineralization (modified by biomacromolecule) and nanocrystallization, respectively[6,7].

For the crystal shape,there are three types of anhydrous crystalline polymorphs of $CaCO_3$, i.e., calcite, aragonite and vaterite[8-11]. Compared with the other two crystalline polymorphs, vaterite is expected to be the most potential material for various purposes due to its good solubility, higher dispersion, larger specific surface area and lower specific gravity[13]. It has been reported that the concentration of carboxyl play an important role in the formation of vaterite[14,15]. Moreover, the using of PASP as organic template can ionize abundant of carboxyl groups on the interface of PASP and Ca^{2+}, and thus promote the formation of vaterite[16].

Water-in-oil (W/O) microemulsion, which is also referred to reverse microemulsion[2,17], has proved to be one of the most effectively preparation method which enables to control the particle properties such as particle size, geometry, morphology, homogeneity and surface area, etc[17-19]. Due to the using of surfactant in the W/O microemulsion, the water is present in the form of nanodroplets and highly dispersed in oil which can be used as nanoreactors to carry out the chemical reactions and thus form the nanoscale materials[16-19]. In addition, the W/O microemulsion method can be combined with the crystal shape modification due tothe presence of water that are essential for the ionizing of PASP. Therefore, the synthesis of nanoscale vaterite $CaCO_3$ can be realized by the combination of W/O microemulsion and biomineralization technology.

Hence, this research was undertaken to demonstrate a novel process for the synthesis of nanoscale vaterite $CaCO_3$ via W/O microemulsion method using PASP as organic template. The effects of different parameters, including the concentration of reactant and additive, on the crystal

* Corresponding author: xiaojige90@126.com

type, particle size and morphology of the $CaCO_3$ were investigated. In addition, the process of interaction between W/O microemulsion and PASP template during the synthesis of $CaCO_3$ will be discussed in detail. It has an important significance on the modification of crystal type and particle size.

2. Materials and Methods

2.1. Materials

The following chemicals were used as received without further purification: calcium chloride ($CaCl_2$, Tianjin Fengchuan Chemical Co., AR), sodium carbonate (Na_2CO_3, Tianjin Fengchuan Chemical Co., AR) as the sources of $CaCO_3$. Sodium alcohol ether sulphate (AES, Tianjin Guangfu Chemical Co., 70%), n-pentanol (Chemical Co., AR), cyclohexane (Chemical Co., AR) were used as surfactant, cosurfactant and oil, respectively. PASP was synthesized via the polymerization of L-aspartic acid in ionic liquid at 200 ^oC as the organic template (as seen in Fig. 1). Ethyl alcohol (Chemical Co., AR), deionized water were used as washing reagent.

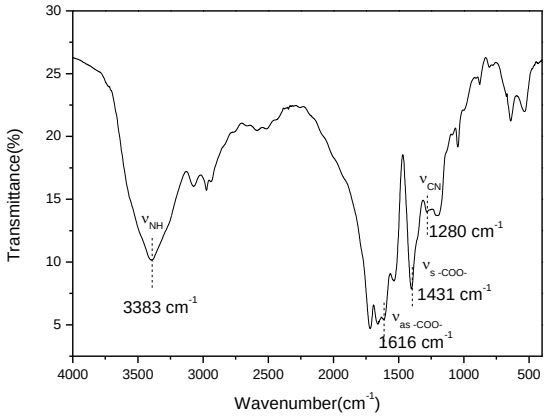

Fig. 1.The FTIR spectrum of PASP.

2.2. Synthesis of $CaCO_3$

Two W/O microemulsions wereprepared by adding a solution of $CaCl_2$ or Na_2CO_3 to the mixture of 28.3 g cyclohexane, 5.9 g AES, 5.9 g n-pentanol, respectively, and stirred for 1 h until the microemulsions became clear and transparent[20]. After that, the two microemulsions were mixed rapidly and reacted for 3 h at 25 ^oC, the obtained white precipitates were separated by centrifugation, rinsed several times with absolute ethanol, dried at 70 ^oC overnight, and finally $CaCO_3$ samples were achieved. The molar ratio of $CaCl_2$ and $Na_2CO_3$was consistently kept at 1:1 with the increasing concentration of two solutions (0.1~0.5M).

To obtain the nanoscale vaterite $CaCO_3$, PASP was used as organic template added into the $CaCl_2$ solution and formed the pre-organization template with Ca^{2+}, the synthesis process was the same as aforementioned method. The concentration of PASP was changed from 0.5 to 2.5 mg/ml to investigate the influence of PASP concentration in the W/O microemulsions on the formation of vaterite.

2.3. Characterization

Samples were collected by X-ray diffraction (XRD) patterns carried out on a Bruker D8 Advance diffractometer using Cu-Kα (k = 1.5406 Å) irradiation with a fixed power source (40 kV, 40 mA) and 2 θ range from 10 ^{o} to 60 ^{o}. The textural and morphological information of the samples were characterized using scanning electronic microscopy (SEM) on a Hitachi S-4800 microscope operated at 30 kV and transmission electron microscopy (TEM) on a JEOLJEM-2010EX microscope with a punctual resolution of 0.23 nm and lineal resolution of 0.14 nm at 20 KV. N_2 adsorption–desorption isotherms of the samples were tested using an Autosorb-iQ apparatus

(Quantachrome Instruments) at 77 K. Prior to the adsorption measurements, all of the samples were out-gassed under a vacuum of 1.33×10^{-3} Pa at 300 °C for 12 h. The impurities remaining on the surface of $CaCO_3$ particles were identified qualitatively by a Fourier transform infrared spectroscopy (Perkin Elmer, Spectrum 100, FT-IR spectrometer).

3. Results

3.1. Structure and morphology

Fig. 2 presents the X-ray diffraction patterns of samples synthesized by different concentration of $CaCl_2$ and Na_2CO_3 solution without using PASP. All of the sample patterns exhibited the characteristic diffraction peaks occurring at 2 θ of 24.91 °, 27.11 °, 32.81 °, 38.61 °, 44.01 °, 49.11 °, 50.21 °, 55.91 ° and 27.04 °, 32.78 °, 43.84 °, 50.07 °, which are exclusively indexed to the structure of calcite and vaterite$CaCO_3$, respectively (JCPDS No. 04-0636 and No. 33-0268)[10], indicates the formation of mixture of two types $CaCO_3$ (Fig. 2a). To investigate changes of the contents of vaterite and calcite, which was obtained at different concentration of $CaCl_2$ and Na_2CO_3 solution, the percentage of each polymorph of $CaCO_3$was calculated from their characteristic reflection peaks intensities by the following equation (eqn 1) according to the results of XRD[10].

$$X_V/X_C = 7.691\ I_V/I_C \quad (1)$$

In eqn 1, X_C and X_V are representative of the molar fractions of calcite and vaterite in the mixture, respectively. The intensities of the peaks of the (104) plane of calcite, and the (110) plane of vaterite are represented as I_C104, and I_V110, respectively. The relationship between computed percentage of vaterite from Fig. 2a and the concentration of reactant was shown in Fig. 2b. It can be seen that the proportion of vaterite was increased with the increasing of reactant concentration in the microemulsion system and almost no longer increased with a maximum value of 75% at the concentration of 0.5M.

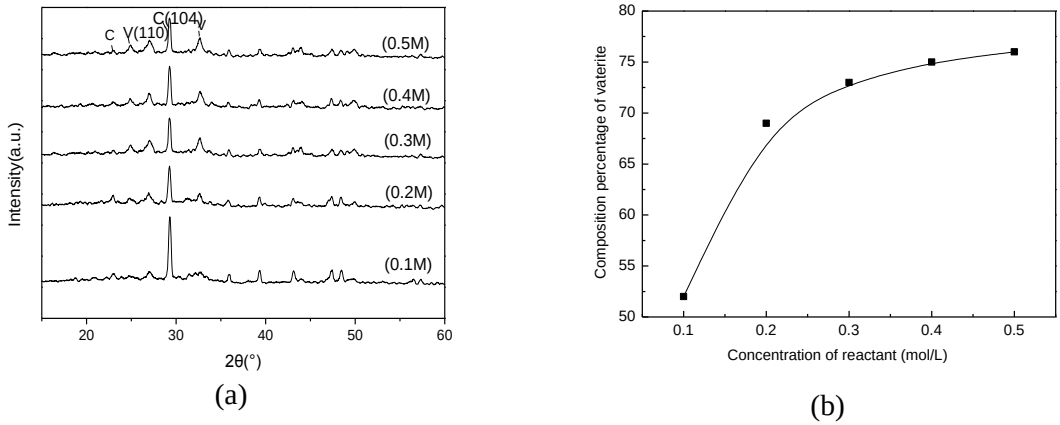

Fig. 2. (a)XRD pattern of $CaCO_3$ and (b) Plot for the percentage of vaterite with reactant concentration

To further increasing the concentration of reactant,the prepared microemulsion was no longer clear due to the demulsification. Therefore, PASP was used as an organic template added into the synthesis system in order to improve the content of vaterite. Fig. 3a illustrates the samples that are synthesized by using different mass concentration of PASP with the reactant concentration of 0.5M. As observed, the content of vateritewas further increased with the increasing of PASP

concentration, and the composition percentage of vaterite crystal of 98.5% was obtained at the PASP concentration of 2.5 mg/ml, as seen in Fig. 3b.

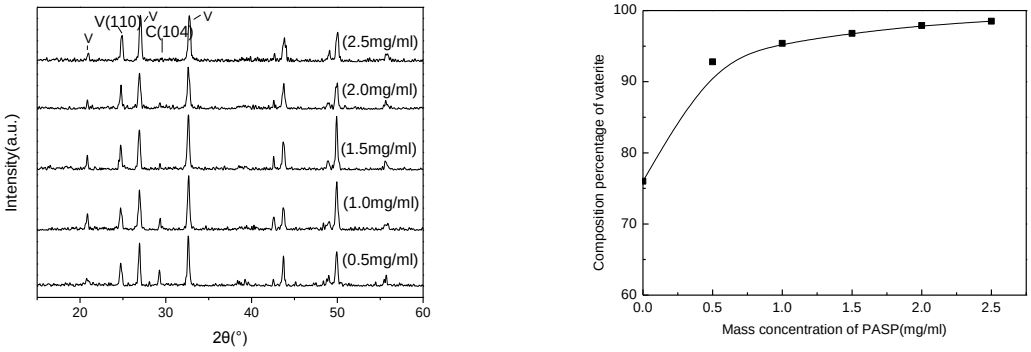

(a) (b)

Fig. 3. (a)XRD pattern of $CaCO_3$ and with PASP mass concentration

Fig. 4 presents the morphologies of the samples that are synthesized under different concentration of 0.1 M and 0.5 M without using PASP as organic template, respectively. As can be seen, both samples were in the form of aggregates consisting of sphere and rhombohedra crystals simultaneously, which are generally indexed to the vaterite and calcite, respectively. Compared with the reactant concentration of 0.1 M, the sample of 0.5 M reactant concentration possessed a higher proportion sphere particles with a smaller size ca.80-100 nm.

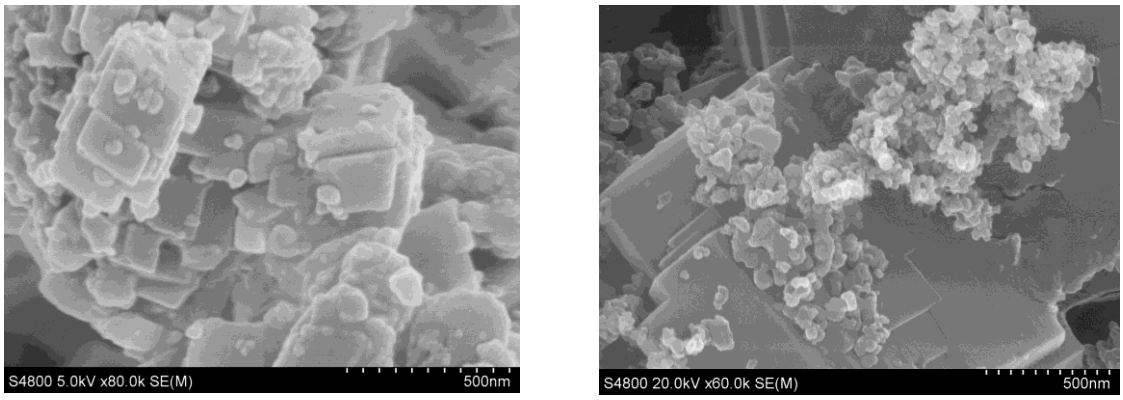

(a) (b)

Fig. 4. SEM photographs of $CaCO_3$ samples synthesized under different reactant concentration: (a)0.1M and (b)0.5M without PASP

The SEM images of samples prepared by adding different concentration of PASP in the reactant system were provided in Fig. 5. It can be seen that both sample were in the form of sphere crystals and no rhombohedra of $CaCO_3$ crystals can be observed. Moreover, the sample prepared of 2.5 mg/ml mass concentration of PASP exhibited a much higher dispersion of sphere particles with a smaller size ca.50 nm. This can be attributed to the production of large number of carboxyl groups on the interface of PASP and Ca^{2+}, which promote the formation of vaterite.

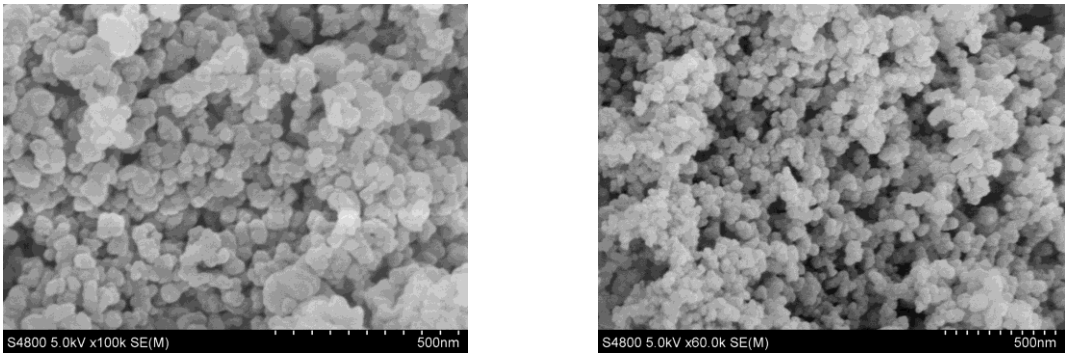

(a) (b)

Fig. 5. SEM photographs of $CaCO_3$ samples synthesized under the PASP concentration of (a)0.5mg/ml and (b)2.5mg/ml

However, the crystal size of ca. 50 nm was larger than that of droplet in typical W/O microemulsion. It may be attributed to the increase of droplet size in the microemulsion[9] as well as the growth and agglomeration of nanocrystalline with the increasing of time. Therefore, samples were synthesized at different reaction time under the PASP concentration of 2.5 mg/ml to study the crystal growth process of vaterite in W/O microemulsion. As can be seen in Fig. 6, both calcite and vaterite were formed at the initial reaction time of 1 h. However, the intensity of the peaks of the (104) plane which belong to calcite was lower than that of vaterite and the composition percentage of vaterite of 96.5% was calculated from eqn 1. Moreover, it can be noted that the half peak width of vaterite became more sharp and the intensity of (110) plane increased with the prolongation of reaction time, which indicated that the crystal size increased.

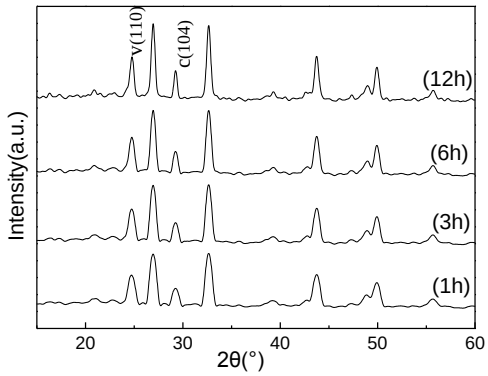

Fig. 6. XRD pattern of $CaCO_3$samples synthesized at different reaction time under the PASP concentration of 2.5mg/ml

To further prove the suggestion, the SEM images of samples synthesized at different reaction time were given in Fig. 7. It can be clearly seen that the $CaCO_3$ samples with smallest crystal size of ca. 10-15 nm was obtained at the initial reaction time of 1 h, which was in accordance with the characterization results of XRD that the intensity of the peaks of vaterite was lowest. With the increasing of reaction time, the nanoscale crystals grew into larger spherical particles and the crystal size was ca 50 nm at the reaction time of 3 h. To further increase the reaction time to 12 h, the crystal size of ca. 100 nm was obtained and the nanoscale vaterite of $CaCO_3$ agglomerated into larger cluster.

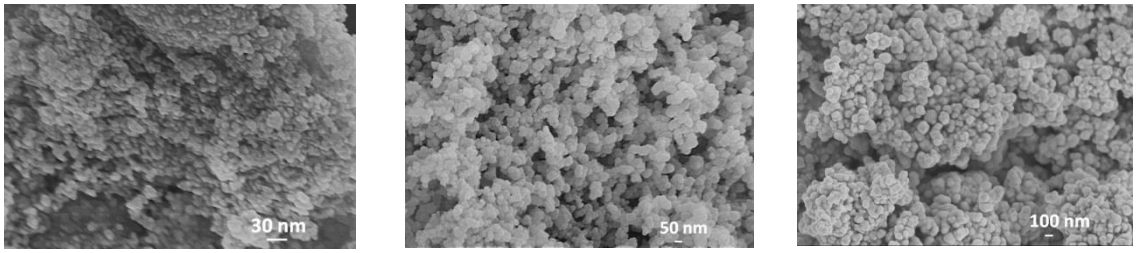

(a) (b) (c)

Fig. 7. SEM photographs of $CaCO_3$ samples synthesized in different reaction time of (a) 1 h (b) 3 h (c) 12 h under the PASP concentration of 2.5mg/ml.

TEM images of the sample synthesized by adding 2.5 mg/ml PASP as organic template at the reaction time of 3 h were shown in Fig. 8. It provided clear clues for the crystal size of the nanoscale spherical particles with a diameter of 50 nm. In the amplified images, the bright region was observed apparently which can be attributed to the presence of mesoporous due to the accumulation of the nanocrystalline and mainly distributed around 40-60 nm. Clear crystal lattice was showed in the further amplification.

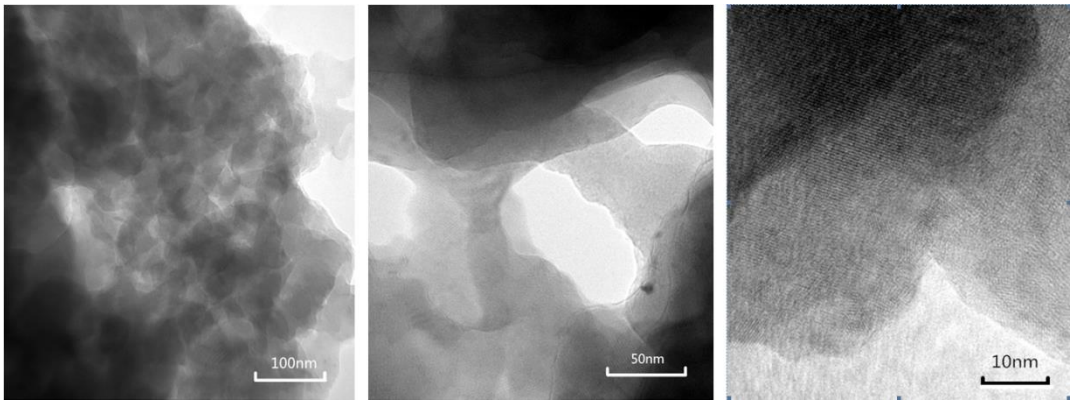

Fig. 8.TEM photographs of the sample synthesized under the PASP concentration of 2.5mg/ml at the reaction time of 3 h.

To investigate the interaction between the surfactant AES and additive PASP, the FTIR analysis was employed. As seen in Fig. 9, the adsorption peaks of 731 cm^{-1} and 1380 cm^{-1} were assigned to C=O which proved the formation of $CaCO_3$[21]. Moreover, both samples show the adsorption peaks corresponding to organic functional groups such as O=S=O (1036 cm^{-1})and S=O (1071 cm^{-1}), suggesting that the surfactant AES strongly adsorbed on the particle surface due to the interaction between anionic surfactant AES and Ca^{2+} cation[22]. However, it's worth noting that the sample synthesized by adding PASP as organic template shows apparent adsorption peaks of 1280 cm^{-1} which corresponding to acylamino groups, the characteristic absorption peak at 1590-1630 cm^{-1} are stretching vibration of C-O bond of amide indicating the PASP connected with the $CaCO_3$ even though extensive washing, which may be attributed to the formation of stable PASP and Ca^{2+}complex[23].

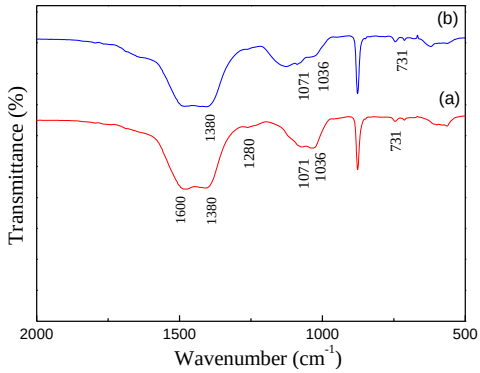

Fig. 9.FTIR spectra of the $CaCO_3$ samples synthesized in W/O microemulsion (a) with PASP or (b) without PASP.

3.2. Textural properties

Fig. 10 provides the N_2 adsorption-desorption isotherms for the sample synthesized by using 2.5 mg/ml mass concentration of PASP at the reaction time of 3 h. As seen in Fig. 10a, the isotherms of the materials are typical IV type isotherms according to the IUPAC classification and exhibit a steadily increasing adsorption amount with the increasing relative adsorption pressure p/p_0, which are characteristic of mesoporous material. Moreover, it also has an apparent hysteresis loop in the range of p/p_0 = 0.45~1.0 which belong to H4 type, implying that there were open mesoporous which formed by the accumulation of nanocrystallines connected to the external surface[24]. Compared with the vaterite $CaCO_3$ refernce to the literature[25] , as shown in Table 1, the surface area and mesoporous volume of nanoscale vaterite $CaCO_3$ sample were improved significantly which achieved of 27.012 m^2/g and 0.15 cm^3/g due to the smaller nanocrystalline size. The broad pore size distribution curve (Fig. 10b) indicates that the nanoscale vaterite $CaCO_3$ had a serious of mesopores with different diameters and mainly distributed around 40~60 nm which was agree with the results from TEM images.

Table 1.Textural data of nanoscalevaterite $CaCO_3$

Samples	**S_{BET}[3] (m^2/g)**	**V_{Total}[4] (cm^3/g)**	**V_{Micro}[5] (cm^3/g)**	**V_{Meso}[6] (cm^3/g)**
Nanoscalevaterite $CaCO_3$[1]	27.012	0.150	0	0.150
Compared vaterite $CaCO_3$[2]	12.266	0.045	0	0.045

[1] synthesized by using of 2.5 mg/ml mass concentration at 0.5 M reactant solution;
[2] reference to the literature [25];
[3] determined by the BET method using adsorption data in p/p_0 ranging from 0.05 to 0.25;
[4]estimated from the adsorbed amount at p/p_0 = 0.99;
[5] measured by t-plot method;
[6]$V_{Meso} = V_{Total} – V_{Micro}$

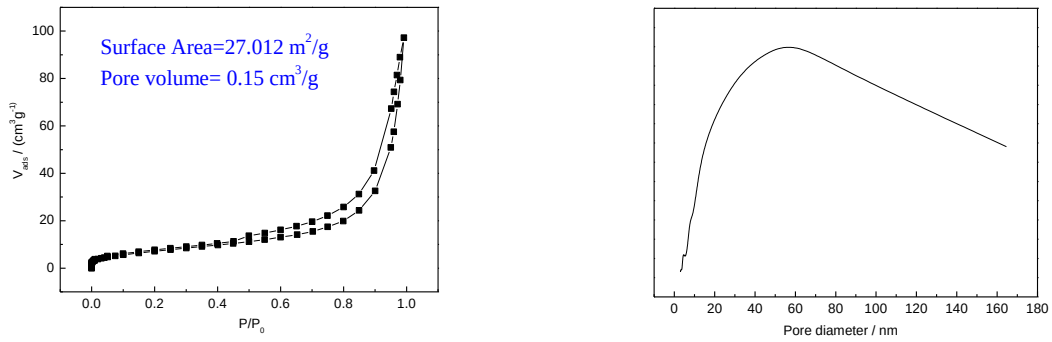

(a) (b)

Fig. 10. (a) N_2 adsorption–desorption and (b)Pore size distribution isotherms at 77 K of the $CaCO_3$ samplesynthesized under the PASP concentration of 2.5mg/ml at the reaction time of 3 h.

4. Discussion

The possible precipitation process of nanoscale vaterite $CaCO_3$ in W/O microemulsion was shown in Scheme. 1. In microemulsion system, because of electrostatic interactions, AES as the anion template would attract Ca^{2+} to the interface edge of the reaction solution and promote the formation of vaterite[26]. Therefore, vaterite nucleation mainly occur at the interface edge of the solution where the template present and calcite nucleation carry out at the internal of solution without the template[27]. When the limited supersaturation has been reached, interface nucleation will be no longer increased which result in the slowly increasing rate of the content of vaterite, as seen in Fig. 2(b). Additionally, the particle size of vaterite became smaller with the increasing of reactant concentration due to the formation of more vaterite crystal nucleus with the samller growth rate. However, the demulsification would be occurred with the further increasing concentration of reactant because of the electrostatic attraction at the interface, so that the nanoscale vaterite would aggregated into large cluster. With the adding of PASP in the W/O microemulsion, -COO^-- ionized from PASP which as the template of vaterite would preferentially bond to Ca^{2+} via the electrostatic attraction and thus prevent the connection with AES. Therefore, the nucleation rate as well as the dispersion of vaterite was promoted due to the suppression of demulsification.

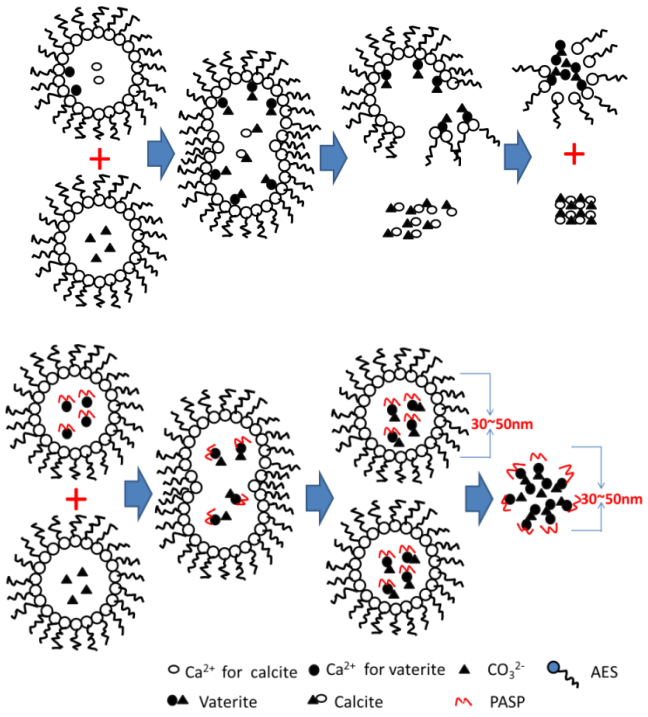

Scheme. 1. The possible precipitation process of nanoscalevateriteCaCO$_3$ in W/Omicroemulsion

5. Conclusions

In this work, the uniform nanoscale vaterite $CaCO_3$ has been obtained successfully by adding the soluble organic template (PASP) into W/O microemulsion. The results of XRD, SEM, TEM, FTIR, N_2adsorption–desorption show that the $CaCO_3$ sample was in the form of aggregates consisting of sphere nanocrystals with a diameter of ca. 50 nm and the pore size distribution was mainly around 40~60 nm due to the accumulation of nanocrystallines. The surface area and mesoporous volume of $CaCO_3$ sample were as high as 27.012 m^2/g and 0.15 cm^3/g, respectively. Furthermore, the regulatory effect of microemulsion and PASP for crystallization process was also examined by the changes of concentration of reactant and PASP. The possible precipitation process of the nanoscale vaterite $CaCO_3$ in the complex system was given. This study makes the synthesis method of nanoscale $CaCO_3$ combine with the theory of biomineralization and provides promising results for the elaboration of a biocompatible material.

Acknowledgments

I would like to extend my sincere gratitude to my teacher, Shilin Yang, for his instructive advice and useful suggestions on my thesis. High tribute shall be paid to Xiaofang Su, whose fluent English improves the language and grammar of the article.

References

[1] H S Liu, K A Chen, C Y Tai,Chem Eng J **197**, 101 (2012).
[2] F W Yan, C Y Guo, X H Zhang, et al,Cryst Eng Comm **14**, 2046 (2012).
[3] X Guo, L Liu, W Wang, et al,Crys tEng Comm **13**, 2054 (2011).
[4] S K Medeiros, E L Albuquerque, F F Maia, et al, Chem Phys Lett **430**, 293(2006).
[5] S M El-Sheikh, S El-Sherbiny, A Barhoum, et al,Colloid Surface A **422**, 44(2013).
[6] R Q Song, H Cölfen, Cryst Eng Comm **13**, 1249 (2011).

[7] A Dey, N A J M Sommerdijk,Chem Soc Rev **39**, 397(2010).
[8] M Saharay, R J Kirkpatrick, Chem Phys Lett **591**, 287(2014).
[9] J Jiang, Y Zhang, D Xu, et al, Cryst Eng Comm **16**, 5221(2014).
[10] H Chen, C Qing, J Zheng, et al, Mat Sci Eng C **63**, 485(2016).
[11] G Hadiko, Y S Han, M Fuji, et al, Mater Lett **59**, 2519(2005)
[12] J Roque, J Molera, M Vendrell-Saz, et al,J Cryst Growth **262**, 543(2004).
[13] H Tong, W Ma, L Wang, et al, Biomaterials **25**, 3923(2004).
[14] B Njegić-Džakula, G Falini, L Brečević, et al,J COLLOID INTERF SCI 343, 553(2010).
[15] A T Nagaraja, S Pradhan M J, McShane,J Colloid Interf Sci **418**, 366(2014).
[16] M A Malik, M Y Wani, M A Hashim,Arab J Chem **5**, 397(2012).
[17] S Thachepan, M Li, S A Davis, et al,Chem Mater **18**, 3557(2006).
[18] K Tong, C Zhao, D Sun, Colloid Surface A **497**, 101(2016).
[19] A M Perez-Coronado, L Calvo, N Alonso-Morales, et al,Colloid Surface A **497**, 28(2016).
[20] L Chiappisi, L Noirez, M Gradzielski, J Colloid Interf SCI **473**, 52(2016).
[21] C K Chen, C Y Tai,Chem Eng SCI **65**, 4761 (2010).
[22] J Chen, L Xu, J Han, et al, Desalination **358**, 42(2015).
[23] F Rauscher, P Veit, K Sundmacher,Colloid Surface A **254**, 183(2005).
[24] K Y Chong, C H Chia, S Zakaria, et al, J Env Che Eng **2**, 2156 (2014).
[25] J Saikia, G Das,J Env Che Eng **2**, 1165(2014).
[26] H Wei, Q Shen, Y Zhao, et al,J Cryst Growth **279**, 439 (2005).
[27] L Liu, D Fan, H Mao, et al,J Colloid Interf SCI **306**, 154 (2007).